

Cautionary Tales of Persistent Accumulation of Numerical Error: Dispersive Centered Advection

Matthew W. Hecht

*Computational Physics and Methods, CCS Division, Los Alamos National Laboratory
Mail Stop B296, Los Alamos, NM, 87545, USA.*

Abstract

We identify a potentially severe source of spurious cooling within and below the thermocline. The effect involves an interplay between tracer advection scheme and eddy parameterization: A dispersive advection scheme generates spurious warm and cold extrema, and then the tracer mixing scheme is relied upon to moderate those extrema. Noise suppression is less robust when the eddy parameterization consists of the more physically based use of eddy-induced transport and isopycnal tracer mixing. Convection occurs in response to the spurious warm and cold extrema generated by the dispersive advection scheme, driving a persistent cooling below the thermocline. When choosing an advection scheme for ocean climate modelling this effect should be considered as a significant concern associated with the use of dispersive centered advection.

Keywords: advection, dispersive error, diapycnal mixing, convection, ocean modelling

1. Introduction

Ocean modelling is fundamentally based upon numerical approximation to continuous equations describing fluid flow, and so numerical error, in the sense of departure from an exact continuum form, is inescapable. Some errors are of course more damaging than others. If an error tends persistently toward a certain sign or effect then it will, over time, accumulate to produce an ever larger bias. In this paper we show that just such a persistent error will tend to arise with use of a dispersive advection scheme, if eddy-induced transport is parameterized following the approach of Gent and McWilliams (1990) (referred to hereafter as GM) and tracer mixing has been rotated into the isopycnal plane (Cox (1987), Redi (1982)).

One would prefer to minimize any source of error, but judgement is required in the choice of which errors to address most aggressively. Errors which contribute to cross-isopycnal mixing are especially important to reduce. Working within a Z-coordinate ocean model, sometimes referred to as a Bryan-Cox-Semtner model, we use GM and isopycnally-oriented tracer mixing in order to reduce the cross-isopycnal error that can so greatly compromise an ocean model, a choice nearly always made in the ocean component of climate models today. In this paper we consider the interplay between the tracer advection scheme and the eddy parameterization. We find that the eddy parameterization allows the error to go unchecked, but it is the advection scheme that is the source of the error in question.

The original ocean model of Bryan (1969) used a second-order centered-in-space and leapfrog centered-in-time discretization. Alternative temporal discretizations have sometimes been adopted in descendants of that model

26 (see for instance the two-time-level implementation described in Griffies et al.
27 (2004) and Griffies (2004), and Hecht (2006) for an overview of forward-
28 in-time methods in ocean modelling), and alternatives to centered-in-space
29 tracer advection are widely available, including those of Gerdes et al. (1991),
30 Holland et al. (1998) and Adcroft et al. (2005), yet centered leapfrog dis-
31 cretizations remain in common use.

32 One explanation for the longevity of the original centered-in-space and
33 leapfrog-in-time approach is the efficiency of the discretization. Cost alone is
34 not, however, the sole issue. The leading-order discretization error of alter-
35 native advection schemes is most often dissipative in character, as contrasted
36 with the dispersive leading error of the centered-in-space scheme. Dispersive
37 error tends to produce grid-scale noise, or oscillations, whereas dissipative er-
38 ror produces excessive smoothing (see Hecht et al. (1995), Hecht et al. (2000)
39 for illustration). Concerns with the introduction of spurious dissipation per-
40 sist. Ocean modelers tend to be particularly reticent to introduce spurious
41 cross-frontal mixing, so as not to short-circuit the large-scale heat transport
42 of the oceans through the Veronis Effect (Veronis (1975)).

43 Notable efforts to quantify levels of implicit dissipation associated with
44 advection schemes include those of Griffies et al. (2000) and Lee et al. (2002).
45 Even with the benefit of quantitative assessments of numerical error, the
46 qualitative impacts of dissipative error raise concerns, as in a recent effort to
47 use a quasimonotonic advection scheme within a global 0.1° version of the Los
48 Alamos Parallel Ocean Program (POP, as described in Maltrud et al. (2010)
49 and references within; the advection scheme was developed by K. Lindsay
50 (private communication)). The jets of the equatorial Pacific were not as well

51 represented as expected, as shown here in Figure 1 (F. Bryan and M. Maltrud,
52 private communication). The specific mechanism through which the jets
53 were degraded was never identified, but replacement of the quasi-monotonic
54 advection scheme with the original centered-in-space scheme was sufficient
55 to address the degradation, recovering a more realistic representation of the
56 jet structure.

57 This example is given in order to illustrate how it is that ocean modelers
58 may still find reason to choose centered-in-space advection. The new finding
59 we present is, however, meant to motivate the reconsideration of alternative
60 schemes. Although ocean modelers have been willing to accept the dispersive
61 error associated with centered advection as the lesser of perceived evils, these
62 errors may not be limited to the generation of isolated, local blemishes, but
63 may instead represent a leading source of spurious cooling.

64 **2. Problematic Results from a Simple Model Configuration**

65 The problem we take up here arose in a simple reentrant zonal channel
66 with a sill, presented in Hecht et al. (2008) in order to evaluate their imple-
67 mentation of the LANS- α turbulence parameterization (Foias et al. (2001)) in
68 the Los Alamos Parallel Ocean Program (Smith et al. (1992), Dukowicz and
69 Smith (1994), Smith and Gent (2002)), an ocean general circulation model
70 based on the primitive equations. Here, we do not consider results from
71 this newer turbulence parameterization, but instead consider the problem-
72 atic results which arise with use of the GM parameterization of eddy-induced
73 transport (see also Danabasoglu et al. (1994), Gent et al. (1995)). When us-
74 ing GM we also rotate the tracer mixing from horizontal to isopycnal planes,

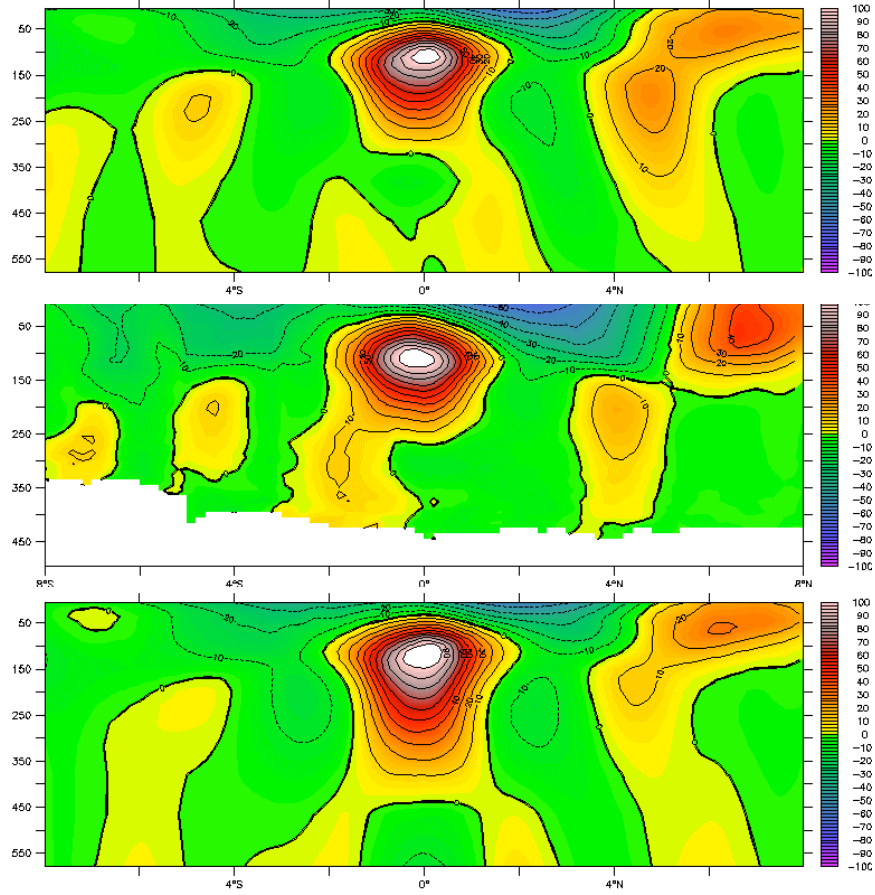


Figure 1: Equatorial Pacific velocities through an upper ocean section at 220°E , (top) from the 0.1° fully global simulation of Maltrud et al. (2010) with centered advection; (middle) from the observations of Johnson et al. (2002); and again (bottom) from the model but with the flux-limited Lax-Wendroff advection scheme of K. Lindsay (private communication). The poorer representation of the equatorial jet structure in the bottom panel, presumably due to the impact of dissipation implicit to the advection scheme, offers one illustration of why ocean modelers may be reticent to adopt alternatives to the centered scheme.

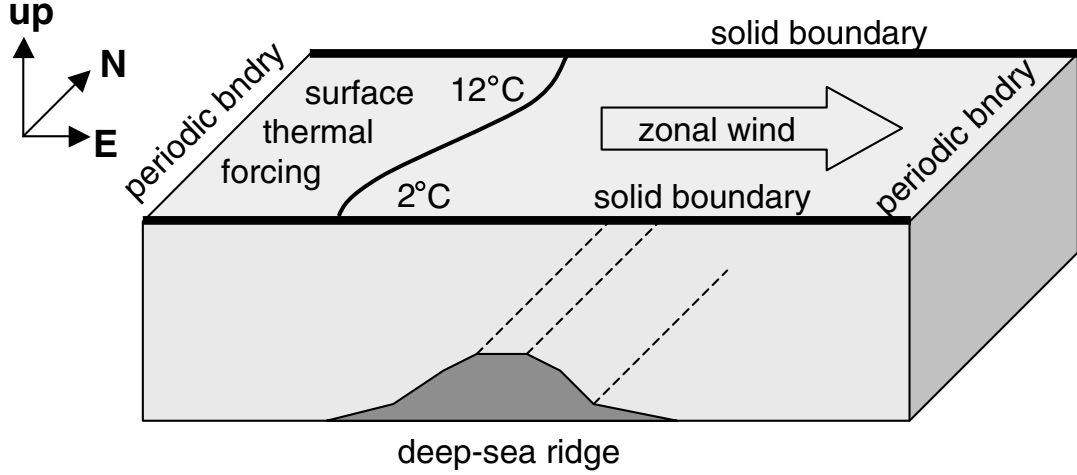


Figure 2: Channel model configuration, as used in and reprinted from Hecht et al. (2008). The zonally-reentrant domain is centered about 60°S . Thermodynamic forcing is thermal only, in the form of a restoring (with time constant of 150 days over 50 meters) to a target temperature varying from 2 to 12°C . Under this forcing, any temperatures of less than 2°C must be spurious.

75 using the same coefficient for the isopycnal tracer mixing as for the eddy-
 76 induced transport.

77 The reentrant channel is an idealized representation of the Southern
 78 Ocean, as shown in Figure 2. The forcing of the model consists of a zonal
 79 wind stress and a simple heat flux based on restoring to the temperature pro-
 80 file indicated in the figure. It is relevant to note that the coldest temperature
 81 to which the model sea surface temperature is nudged is 2°C .

82 The model domain spans 16° in latitude, centered about 60°S , and for
 83 computational efficiency the flow is reentrant after only 32° of longitude. In
 84 all of the cases shown here the model resolution is 0.4° in latitude and 0.8° in
 85 longitude, providing a nearly uniform aspect ratio in terms of zonal to merid-

86 ional grid spacings. The implementation of GM eddy-induced transport and
87 the associated isopycnal tracer mixing used here is based on the more effi-
88 cient "skew-flux" form introduced in Griffies (1998), and is limited to isopy-
89 cnal slopes less than 1%. Other relevant parameterizations include a simple
90 Richardson number-dependent vertical mixing scheme (Pacanowski and Phi-
91 lander (1981)) and convective mixing through enhanced vertical mixing in
92 response to static instability. Initially, we use the second-order centered-in-
93 space discretization of advection.

94 The problem that faces us is that of understanding an extraordinary,
95 pathological cooling that appears when we switch from horizontal biharmonic
96 mixing of tracers to the use of GM and isopycnal tracer mixing. This extreme
97 cooling is evident even in a volume-mean time series of potential temperature,
98 as in the lower-most curve of Figure 3. The initial point on this time series
99 is the equilibrium value produced by the model as configured in the control
100 case of Hecht et al. (2008), with horizontal biharmonic tracer mixing.

101 Some degree of cooling was expected with the transition from horizontal
102 tracer mixing to GM. Within 175 years, however, a cell appears, at depth
103 and against the sill, which is actually colder than the coldest temperature
104 to which the surface is nudged. It is not unknown for ocean models to
105 produce pathologically cold temperatures if the tracer advection scheme is
106 not monotonic. Here, however, the entire deep ocean cools to unrealistically
107 cold values as the simulation is extended through a few more centuries. After
108 approximately 425 years, the volume-mean potential temperature itself falls
109 below the range of temperatures produced by the surface forcing.

110 Before going on to identify the mechanism behind this pathological cool-

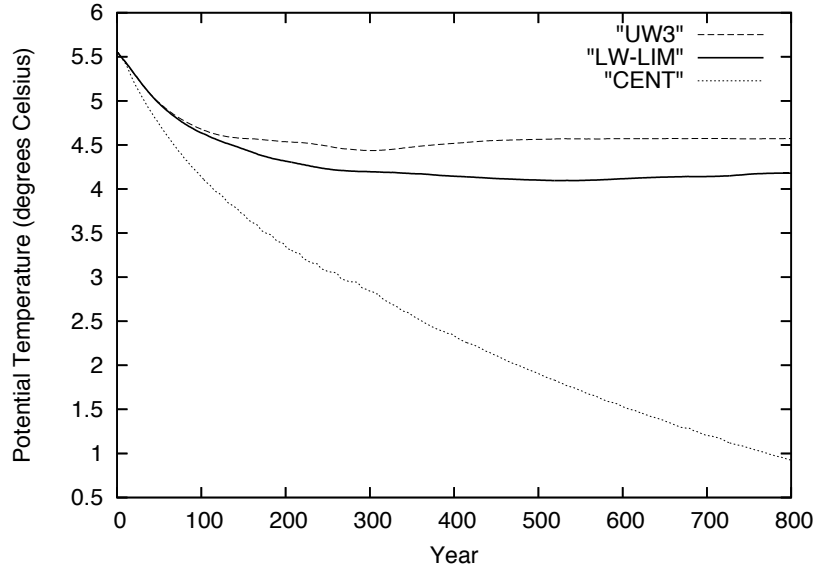


Figure 3: Volume-mean potential temperature as a function of time from integrations with three different tracer advection schemes. The lower curve was produced with centered differencing, the upper curve with the third-order upwind scheme of Holland et al. (1998), and the middle curve with the flux-limited Lax-Wendroff advection scheme of K. Lindsay (private communication). The cooling seen in the third-order upwind and flux-limited cases is due to the physical effect of parameterized eddies (the initial condition had been produced without use of the GM parameterization), whereas the spurious cooling of the centered differencing case is the subject of this paper.

111 ing, we comment further on the model state. After 800 years of model inte-
112 gration, toward the end of the time series of Figure 3, one cell in the model
113 domain has a temperature of less than -1°C , fully 3° beneath the coldest
114 value to which the surface is nudged. In Figure 4, this cell is found to be
115 located against the sill, nearly but not quite at the deepest model level. Wa-
116 ters colder than the coldest surface nudging value of 2°C fill the entire depth
117 of the ocean below 1000 meters.

118 A horizontal slice at depth, containing the coldest cell, is shown in Fig-
119 ure 5. The strongest velocities are in the lee of sill, and the coldest cell lies at
120 a point of convergence, where the vertical velocity is consequently determined
121 to be upwards.

122 Despite the extreme cooling at depth, the surface and near-surface waters
123 remain reasonably warm. The average surface temperature is in fact slightly
124 warmer than in the control case of Hecht et al. (2008), and the enhanced
125 outgoing surface heat flux allowed for by this slight increase in sea surface
126 temperature correctly accounts for the overall domain-averaged cooling.

127 An inspection of advective and diffusive tendencies acting on the coldest
128 cell indicates that the advective term is causing this coldest point to become
129 colder yet (note that advection does not include a bolus velocity contribution,
130 as we are using the skew-flux form of the tracer mixing parameterization).
131 When we replace the centered advection with a quasi-monotonic form of the
132 Lax-Wendroff scheme (as above, K. Lindsay, private communication) and
133 repeat the simulation, the volume mean temperature drops only modestly,
134 as seen in the time series represented by the solid line of Figure 3. This drop
135 in mean temperature is only what one would expect with use of GM (it is the

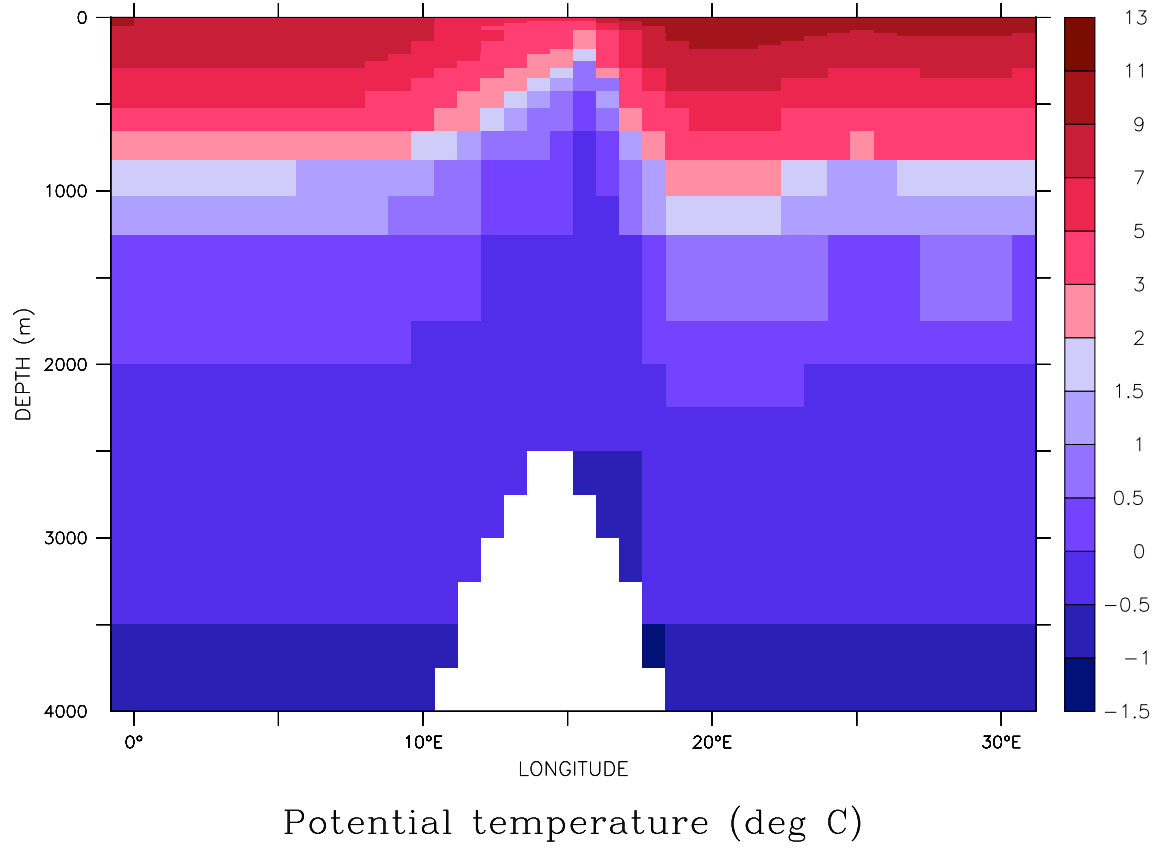
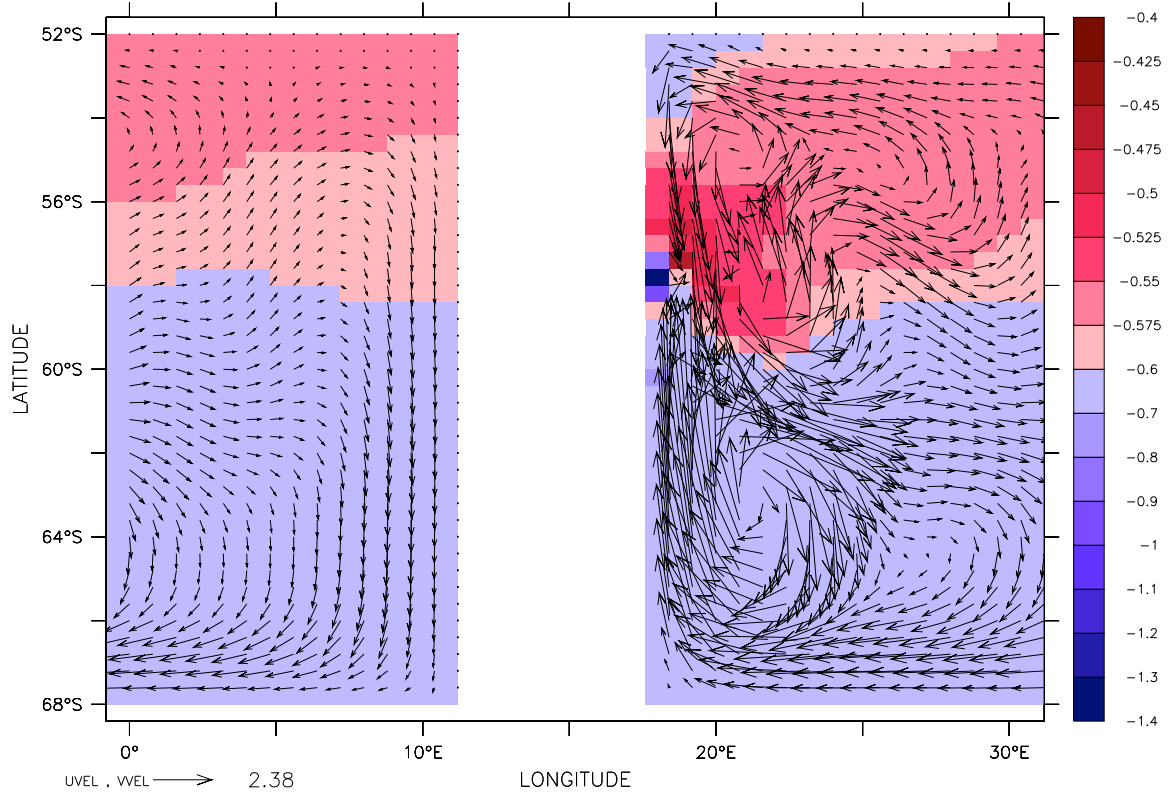


Figure 4: A zonal section of potential temperature at 55.8°S , at model year 800. One cell in the model domain has a temperature which has fallen below -1°C ; this coldest cell is located one level up from the deepest model level. All waters shaded in blue have become colder than any temperature to which surface waters are nudged, and have been produced instead through dispersive numerical effects.



Potential temperature (deg C)

Figure 5: A horizontal section within the next-to-deepest level, centered about 3625m, and at year 800. The coldest cell is located just above the last step of the sill (as evident in the profile view of Figure 4). Velocity vectors are drawn over the potential temperature field.

136 bolus velocity term, represented here through the antisymmetric component
137 of the mixing tensor (Griffies (1998)), which tends to flatten isopycnals and
138 causes this more moderate and physically based cooling). The potential
139 temperatures also remain within reasonable bounds when we use the so-
140 called third-order upwind scheme of Holland et al. (1998), as indicated by
141 the dashed curve of Figure 3.

142 The vertical dependence of extreme cooling is more readily discerned in
143 Figure 6. Level-averaged temperatures first fall below 2°C , the lower limit of
144 the range of surface forcing, around year 200. Waters above 250m show little
145 drift in temperature, indicating that vertical heat transports contribute little
146 net divergence there, even if heat passes through en route to the surface,
147 where it can be dissipated. At levels below 1000 m persistent loss of heat
148 occurs, even as the minimum temperature of the forcing is greatly exceeded.

149 **3. Discussion**

150 The advective tendency, not the diffusive tendency, was identified as caus-
151 ing the coldest point to become colder yet. Ordinarily, a diffusive term of
152 Laplacian form might be assumed to stay within the bounds of monotonicity,
153 so long as a time step limit were not exceeded, but with the skew-flux form of
154 GM departures from monotonicity may occur (Griffies et al. (1998), Griffies
155 (1998)), and so this question of attribution to advective or diffusive tendency
156 arose.

157 Colder waters at depth tend to remain at depth, and so one extremely
158 cold cell, located at the next-to-bottom model level, will not drive the entire
159 ocean below 1000 meters to such cold temperatures. The explanation for the

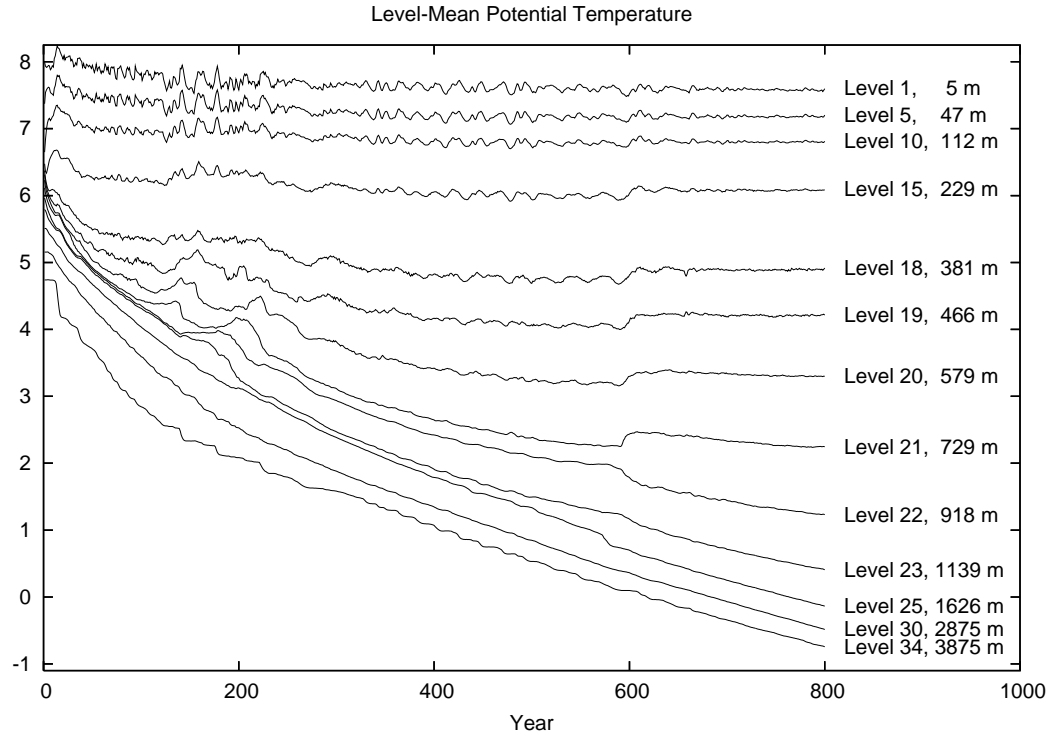


Figure 6: Level-averaged potential temperature as a function of time. Waters above 250m show little drift in potential temperature. At levels below 1000m pathological cooling occurs unabated, even after 800 years.

160 larger-scale cooling of the deep ocean must address how pathologically cold
161 waters may form at the thermocline and below, and must also explain how
162 the surface comes to be anomalously warm, if only slightly so, allowing for
163 a persistent enhancement of the outgoing heat flux that paces the domain-
164 averaged cooling.

165 As discussed in the Introduction, the leading-order numerical error pro-
166 duced by the centered advection scheme is dispersive in character, rather
167 than dissipative. This is to say that it tends to produce spurious ripples, or
168 grid-scale noise, as opposed to spurious smoothing. The dispersive error will
169 tend to make one cell overly warm, but only while making an adjacent cell
170 overly cold.

171 It is dispersive error of just this sort that produces pairs of anomalously
172 warm and cold waters, adjacent to one another, which may then separate
173 vertically under the model response to static instability, cooling the deep
174 ocean and warming the surface. The dispersive generation of error can be
175 expected to be largest where velocities and tracer gradients are large, in the
176 thermocline.

177 If static instabilities are not mixed away but are allowed to remain, then
178 this dispersive generation of hot and cold cells become visible. In the upper
179 panels of Figure 7 the change in tracer concentration over a single model step
180 is shown, with convection suppressed (the section is at the same location as
181 that of Figure 4). The largest changes are seen not at the location of the
182 coldest cell, at depth, but in the thermocline where velocities and tracer
183 gradients are both high.

184 Inspection of the vertical convective response to the sum of all other

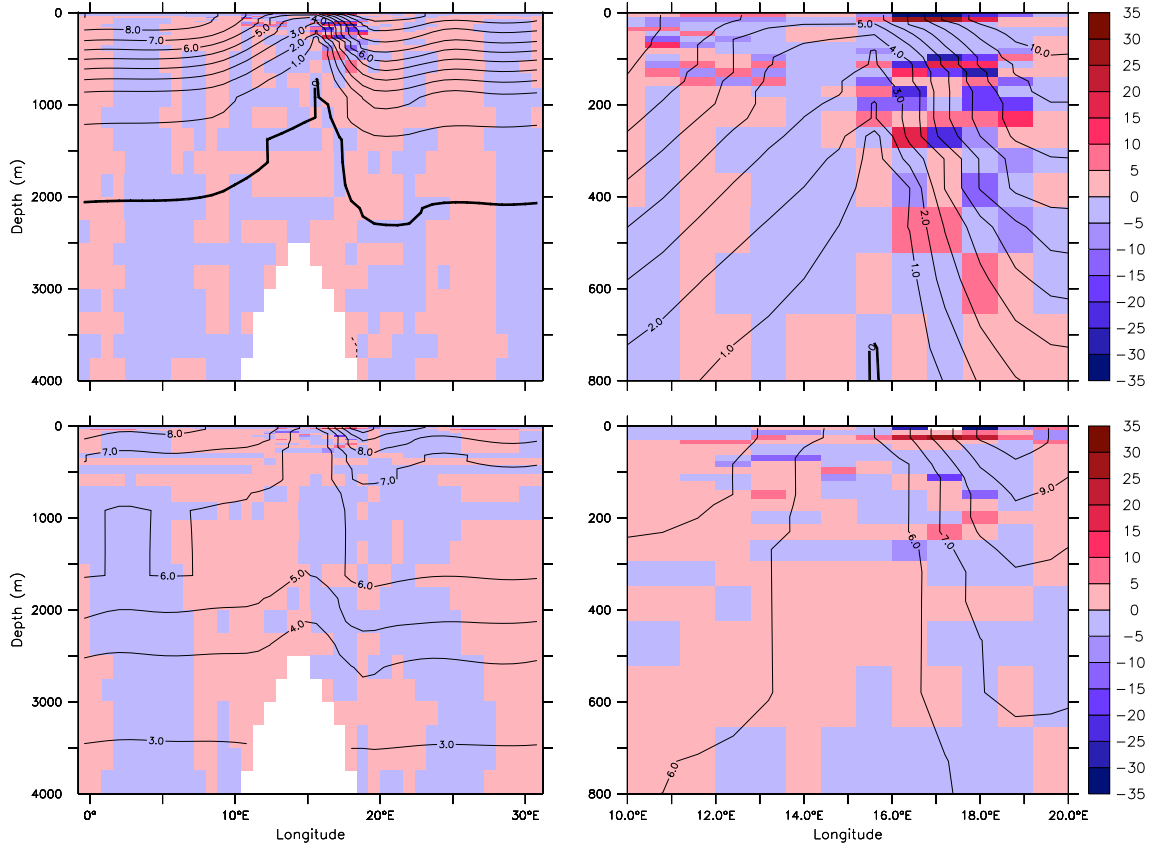


Figure 7: Temperature tendency evaluated over a model time step, with convective response to static instability suppressed for this one step (units are millikelvin per model step of 7200 seconds). The problematic case with centered differencing is shown at top, with magnified view at upper right. The section is taken at 57.8°S , the latitude at which the coldest point in the domain is found at this time of 800 years. Potential temperature is drawn over the tendency field with a contour interval of 1°C . The case produced with third-order upwinding, at bottom, exhibits far less generation of dispersive numerical error on which vertical convection might act.

185 tendencies confirms that convection works to take anomalously cold waters
186 down, and to take anomalously warm waters upwards (the convective re-
187 sponse is not shown here, but is consistent with the response expected to the
188 tendencies of Figure 7). Each dispersively-generated source of warm water
189 need not necessarily transport that warmth all the way to the surface in one
190 continuous action. Collectively, the many sources of warm water contribute
191 to produce a spurious transport of heat toward the surface. These individual
192 sources of anomalous warmth are paired with sources of anomalously cold
193 water, as the advection scheme is conservative. The overall process through
194 which dispersive advective error drives the spurious upward transport of heat
195 involves anomalously warm cells which trigger upward convection and anoma-
196 lously cold cells driving downward convection, with both contributing to the
197 spurious upward heat flux, producing ever colder deep waters.

198 The extreme cooling seen here is not caused by the use of GM eddy-
199 induced transport and isopycnal tracer mixing. The cooling appears because
200 these parameterizations are not as capable of controlling the dispersive error
201 produced by the advection scheme, as compared with the use of a simple and
202 more spatially uniform horizontal tracer mixing. Formally, this requirement
203 for a certain minimum level of dissipation in order to ensure the control of
204 grid scale noise is discussed in terms of a grid-Peclet number constraint in
205 Griffies (2004) (Peclet number being the analog of Reynolds number, but
206 for scalar transport). The issue is illustrated by Hecht et al. (1995), where
207 the observation is made that domain-wide control of grid scale noise may re-
208 sult in excessive smoothing of the transported field. The greater potential for
209 Peclet number violation with the use of GM and isopycnal tracer mixing, and

210 the concern for "contamination" of water masses, was raised in the appendix
 211 of Hirst and McDougall (1996), where they make the point that solutions
 212 should be checked carefully for such contamination. The potential for a dis-
 213 persive advection scheme to spuriously enhance the density contrast between
 214 upper ocean and abyss was commented on by Griffies et al. (2000), and here
 215 we have seen the potential magnitude of the effect. The ocean component
 216 of a newer version of a previously documented coupled climate model, the
 217 Fast Ocean Rapid Troposphere Experiment of Sinha and Smith (2002) and
 218 Smith et al. (2004), is also reportedly affected by a similar cooling at depth,
 219 apparently due to the same mechanism investigated here (A. Blaker, private
 220 communication).

221 The third-order upwind scheme we consider as an alternative to centered
 222 differencing is not a monotonic scheme, and may produce considerable over-
 223 or under-shoots. The upwind-biasing of the solution, however, reduces the
 224 dispersive character of the scheme. In the lower panels of Figure 7 the ten-
 225 dency field produced with the third-order upwind case is shown, again with
 226 convective response to static instability suppressed. The dispersive produc-
 227 tion of warm and cold cells is much reduced, relative to what is seen in the
 228 problematic centered differencing case, and the spurious vertical transport
 229 and secular cooling of the intermediate and deep ocean is consequently much
 230 reduced.

231 There is one aspect of our problem that presents an extreme challenge to
 232 the use of GM and isopycnal mixing with a noisy advection scheme. With
 233 uniform salinity, as in this problem, isopycnal surfaces are coincident with
 234 isothermal surfaces, and the isopycnal mixing term is incapable of providing

any suppression of noise in the potential temperature field. When a weak variability in salinity is introduced, however, our result still holds. For instance, with an overall variability of 0.1 ppt the spurious cooling is very nearly unaffected. One sees a significant reduction in the overall cooling rate when a more typical oceanic variability of 1.0 ppt is specified, and yet one can be assured that pairs of anomalously warm and cold cells are still being created at every time step by the dispersive advection scheme. At any of these places where the equation of state is dominated by potential temperature, this dispersive error will then drive spurious convection. Violations of grid-Peclet number constraint are more severe when GM and isopycnal tracer mixing are used, and it should now be understood that this violation results in a spurious upward heat flux.

4. Conclusion

The results shown here were produced in an idealized context, with simple forcing and topography, and yet the conditions responsible for the persistent accumulation of error are found in ocean climate models. In those places in which velocities and tracer gradients are high one must expect a spurious upward heat flux to occur, so long as a highly dispersive advection scheme is used along with isopycnal tracer mixing. It may be difficult in the more realistic context to identify the extent to which dispersive error biases the water properties in an ocean climate model, where deficiencies in surface forcing and large scale circulation must also be considered, and where numerical error may not necessarily drive a water mass beyond obvious physical bounds, but such errors must be expected to bias sub-thermocline waters towards

259 colder temperatures.

260 One hazard incurred with use of upwind-weighted advection schemes is
261 well known to ocean modelers. Under the Veronis Effect spurious diapycnal
262 mixing across a front presents a sort of short-circuit to the large-scale heat
263 transport (Veronis (1975), Böning et al. (1995)). Less well understood issues
264 such as that illustrated in Figure 1 also present a concern regarding use of
265 schemes with leading-order numerical error of dissipative form. Here we have
266 shown that dispersive error, or the rippling produced by a spatially-centered
267 advection scheme, cannot be dismissed as a merely cosmetic concern, but may
268 also introduce a significant bias, in this case toward a colder ocean below the
269 thermocline. Hirst and McDougall (1996) called for careful inspection of
270 solutions to identify this sort of numerical contamination of water masses.
271 We call for the prudent elimination of the source of numerical contamination
272 represented by the use of second-order centered-in-space advection.

273 A numerical error which violates the second law of thermodynamics in
274 such a persistent way, through creation of spurious dispersive warm and
275 cold extrema which then drive a secular cooling, is a particularly damaging
276 type of error. Nevertheless, one should not simply trade the hazards of one
277 error for those of another, and so a renewed effort must be mounted to gain
278 confidence in the use of better tracer advection schemes in ocean modelling so
279 as to minimize the spurious cross-frontal mixing associated with dissipative
280 error while also eliminating the spurious cooling that is a consequence of
281 uncontrolled dispersive error.

282 5. Acknowledgments

283 We thank Mathew Maltrud and Frank Bryan for the result shown in
284 Figure 1 and Gokhan Danabasoglu for comments on the manuscript. The
285 ideas presented here were developed in conversation with the other ocean
286 modelers at Los Alamos. This work was supported by the Department of
287 Energy’s Office of Science. Los Alamos National Laboratory is operated by
288 Los Alamos National Security, LLC for the Department of Energy.

289 References

- 290 Adcroft, A., Campin, J., Heimbach, P., Hill, C., Marshall,
291 J., 2005. MIT-gcm manual. Technical Report. MIT.
292 http://mitgcm.org/pelican/online_documents/manual.html.
- 293 Böning, C.W., Holland, W.R., Bryan, F.O., Danabasoglu, G., McWilliams,
294 J.C., 1995. An overlooked problem in model simulations of the thermoha-
295 line circulation and heat-transport in the Atlantic Ocean. *J. Clim.* 8, 515
296 – 523.
- 297 Bryan, K., 1969. A numerical method for the study of the circulation of the
298 World Ocean. *J. Comput. Phys.* 4, 347–376.
- 299 Cox, M., 1987. Isopycnal diffusion in a z-coordinate ocean model. *Ocean*
300 *Modelling* 74, 1–5.
- 301 Danabasoglu, G., McWilliams, J.C., Gent, P.R., 1994. The role of mesoscale
302 tracer transports in the global ocean circulation. *Science* 264, 1123–1126.

303 Dukowicz, J.K., Smith, R.D., 1994. Implicit free-surface method for the
304 Bryan-Cox-Semtner ocean model. *J. Geophys. Res.* 99, 7,991—8,014.

305 Foias, C., Holm, D.D., Titi, E.S., 2001. The Navier-Stokes-alpha model of
306 fluid turbulence. *Physica D: Nonlinear Phenomena* 152-153, 505 – 19.

307 Gent, P.R., McWilliams, J.C., 1990. Isopycnal mixing in ocean circulation
308 models. *J. Phys. Oceanogr.* 20, 150—155.

309 Gent, P.R., Willebrand, J., McDougall, T.J., McWilliams, J.C., 1995. Pa-
310 rameterizing eddy-induced tracer transports in ocean circulation models.
311 *J. Phys. Oceanogr.* 25, 463–474.

312 Gerdes, R., Koberle, C., Willebrand, J., 1991. The influence of numerical
313 advection schemes on the results of ocean general circulation models. *Clim.*
314 *Dyn.* 5, 211—226.

315 Griffies, S., 1998. The Gent-McWilliams skew-flux. *J. Phys. Oceanogr.* 28,
316 831–841.

317 Griffies, S., Pacanowski, R., Hallberg, R., 2000. Spurious diapycnal mixing
318 associated with advection in a z-coordinate ocean model. *Mon. Weather*
319 *Rev.* 128, 538–564.

320 Griffies, S.M., 2004. *Fundamentals of Ocean Climate Models*. Princeton
321 University Press.

322 Griffies, S.M., Gnanadesikan, A., Pacanowski, R.C., Larichev, V.D., Dukow-
323 icz, J.K., Smith, R.D., 1998. Isonutral diffusion in a z-coordinate ocean
324 model. *J. Phys. Oceanogr.* 28, 805 – 830.

325 Griffies, S.M., Harrison, M.J., Pacanowski, R.C., Hallberg, R.W., 2004.
 326 A technical guide to MOM4. GFDL Ocean Group Technical Report
 327 5. NOAA/Geophysical Fluid Dynamics Laboratory. Available on-line at
 328 <http://www.gfdl.noaa.gov/~fms>.

329 Hecht, M.W., 2006. Forward-in-time upwind-weighted methods in ocean
 330 modelling. *Int. J. Numer. Meth. Fl.* 50, 1159–1173.

331 Hecht, M.W., Holland, W.R., Rasch, P.J., 1995. Upwind-weighted advec-
 332 tion schemes for ocean tracer transport: An evaluation in a passive tracer
 333 context. *J. Geophys. Res.* 100, 20763—20778.

334 Hecht, M.W., Holm, D.D., Petersen, M.R., Wingate, B.A., 2008. Implemen-
 335 tation of the LANS-alpha turbulence model in a primitive equation ocean
 336 model. *J. Comput. Phys.* 227, 5691–5716.

337 Hecht, M.W., Wingate, B.A., Kassis, P., 2000. A better, more discriminating
 338 test problem for ocean tracer transport. *Ocean Modelling* 2, 1–15.

339 Hirst, A., McDougall, T., 1996. Deep-water properties and surface buoy-
 340 ancy flux as simulated by a z-coordinate model including eddy-induced
 341 advection. *J. Phys. Oceanogr.* 26, 13201343.

342 Holland, W.R., Bryan, F.O., Chow, J.C., 1998. Application of a third-order
 343 upwind scheme in the NCAR Ocean Model. *J. Clim.* 11, 1487—1493.

344 Johnson, G.C., Sloyan, B.M., Kessler, W.S., McTaggart, K.E., 2002. Direct
 345 measurements of upper ocean currents and water properties across the
 346 tropical Pacific during the 1990’s. *Prog. Oceanogr.* 52, 31–36.

347 Lee, M.M., Coward, A.C., Nurser, A.J.G., 2002. Spurious diapycnal mixing
 348 of the deep waters in an eddy-permitting global ocean model. *J. Phys.*
 349 *Oceanogr.* 32, 1522 – 1535.

350 Maltrud, M., Bryan, F., Peacock, S., 2010. Boundary impulse response func-
 351 tions in a century-long eddying global ocean simulation. *Environmental*
 352 *Fluid Mechanics* 10, 275–295.

353 Pacanowski, R., Philander, S., 1981. Parameterization of vertical mixing in
 354 numerical models of tropical oceans. *J. Phys. Oceanogr.* 11, 1443–1451.

355 Redi, M.H., 1982. Oceanic isopycnal mixing by coordinate rotation. *J. Phys.*
 356 *Oceanogr.* 12, 1154 – 1158.

357 Sinha, B., Smith, R., 2002. Development of a fast Coupled General Circu-
 358 lation Model (FORTE) for climate studies, implemented using the OASIS
 359 coupler. Internal Document 81. Southampton Oceanography Centre. 67pp.

360 Smith, R.D., Dukowicz, J.K., Malone, R.C., 1992. Parallel ocean general
 361 circulation modeling. *Physica D: Nonlinear Phenomena* 60, 38–61.

362 Smith, R.D., Gent, P., 2002. Reference manual of the Parallel Ocean Pro-
 363 gram (POP). Los Alamos National Laboratory report LA-UR-02-2484.
 364 Los Alamos National Laboratory. Los Alamos, NM.

365 Smith, R.S., Dubois, C., Marotzke, J., 2004. Ocean circulation and climate
 366 in an idealised Pangean OAGCM. *Geophys. Res. Lett.* 31, L18207.

367 Veronis, G., 1975. Numerical Models of Ocean Circulation. *Natl. Acad. Sci.*,

368 Washington, D.C.. chapter The role of models in tracer studies. pp. 133–
369 146.